

Utilization of high resolution satellite geoid data for estimation of lithospheric thickness in the Bay of Bengal

T J Majumdar^{1*}, R Bhattacharyya¹, S Chatterjee¹ & K S Krishna²

¹Earth Sciences and Hydrology Division, Marine and Earth Sciences Group, Remote Sensing Applications Area, Space Applications Centre (ISRO), Ahmedabad 380 015, India

²National Institute of Oceanography, Council of Scientific & Industrial Research, Dona Paula, Goa – 403 004, India
*[E-mail: tjmajumdar@rediffmail.com]

Received 15 May 2008; revised 22 June 2009

Very high-resolution database generated from Seasat, Geosat GM, ERS-1 and TOPEX/ POSEIDON altimeters data of the northern Indian Ocean has been used for the first time for preparation of geoid and free-air gravity maps. In the present work, geoid height anomalies have been analyzed across the Ninetyeast and 85°E Ridges within the Bay of Bengal. Present data sets are more accurate and detailed (off-track resolution: about 3.33 km and grid size: about 3.5 km). Observed geoid height – age and geoid height derivative (with respect to age) – age relationships have been established and compared with the plate model of lithospheric cooling to determine. The present endeavor is to determine the lithospheric plate thickness beneath both ridge structures. Attempts have been made to match the observed value with the computed value over the Bay of Bengal. The lithospheric plate cooling model correlates convincingly with the observed value. It has shown the efficacy of a plate model according to which geoid observations of the Bay of Bengal are better explained by a larger plate thickness of 90 – 125 km for the oceanic crust of age older than 30 Ma.

[Key Words: Satellite Geoid, Lithospheric Thickness, Geosat GM, ERS-1, Bay of Bengal, 85° E Ridge, Ninetyeast Ridge]

Introduction

Satellite altimetry has emerged as a powerful reconnaissance tool for exploration of sedimentary basins on Indian continental margins and deep-water regions^{1,2}. The very high resolution Geosat GM (Geodetic Mission) data along with Seasat, ERS-1 and TOPEX/POSEIDON altimeter data can generate a very high-resolution data with a grid of around 3.5 km^{3,4}. This data would be very helpful in extraction of minute geological details over the Indian offshore. The sea surface height measured by satellite altimeter, when corrected for atmospheric propagation delays and dynamic oceanic variabilities, conforms to the equipotential surface, known as the geoid (Fig. 1). Geoid is used to compute residual and prospecting geoids - hypothetical surfaces related to the mass distribution at various depths within the lithosphere⁵.

The lithosphere — asthenosphere boundary is a rheological boundary dependent upon temperature. At the ridge axis, the base of the lithosphere is almost close to the surface. As the lithosphere cools, the boundary moves downward, making the lithosphere thicker. The large-scale topography of the ocean floor, therefore, reflects the underlying thermal state of the

lithosphere which correlates directly with its age that is younger than 60-80 Ma. For older ages, the lithosphere does not continue to thicken, nor does the depth of the ocean bottom continue to increase; indicating that a thermal steady state has been reached in the lithosphere which permits the steady conductive outflow of heat from the Earth's interior⁶⁻⁸.

As far as the thermal structure of the lithosphere is concerned, a simple model has been proposed to explain cooling and contraction as the plate expands away from the ridge crest. The plate model is preferred because both depth and heat flow data follow the behavior predicted by the theory, in approaching an asymptotic value in the older parts of the ocean basins⁹. Residual geoid observations are very sensitive to the bottom boundary conditions, particularly for thermal models.

Residual geoid anomalies had been analysed over the Ninetyeast and 85°E Ridges in the Bay of Bengal. Together with seafloor ages, we have estimated the change in residual geoid height with age, geoid slope – age relationship as well as its derivative with respect to age. Geoid anomalies observed over the Ninetyeast and 85°E Ridges show a variation in amplitude. Since

it is reasonable to assume that in ridge zones geoid offset occurs because the portions of lithosphere on each side of the ridge zones have different thickness and density structures as predicted by the thermal models of geoid offset^{7,8}. The residual geoid anomaly can be directly related to the change in lithosphere and to its thermal isostatic compensation at the base of the plate⁹⁻¹¹.

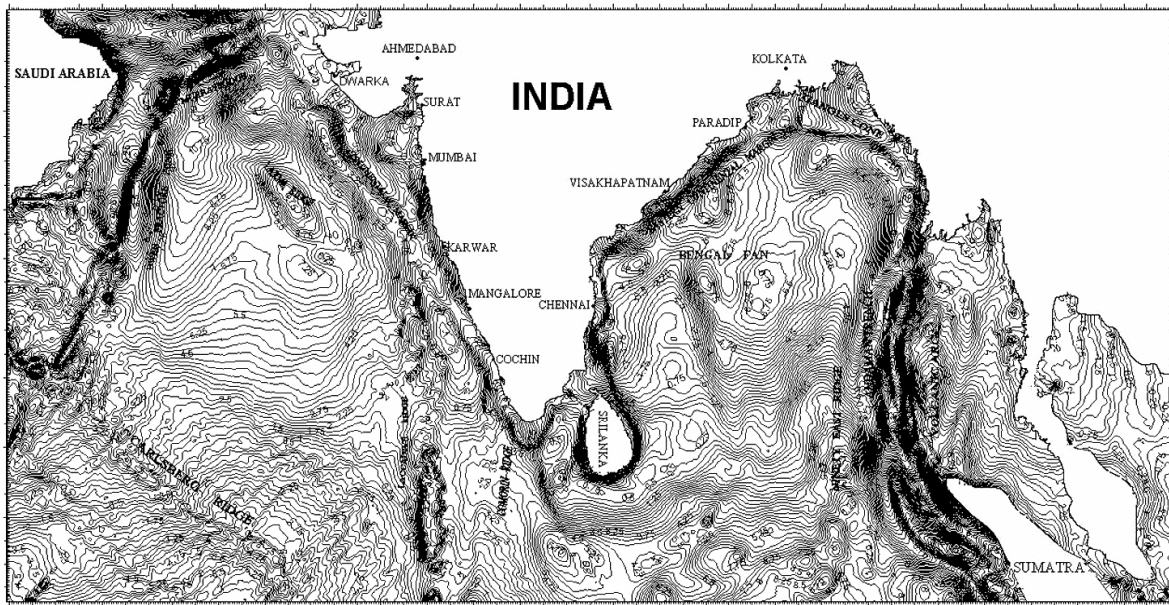
Materials and Methods

The geoid data has been generated using high density data base obtained from Geosat GM (Geodetic Mission), ERS-1, TOPEX/POSEIDON, and Seasat altimeter data over the Indian offshore (Fig. 1)³. Because of being high density in nature (off-track resolution~ 3.33 km), sea surface parameters as well as gravity derived from these data are more accurate and detailed. Details of altimeter data and their preprocessing have been discussed elsewhere^{2,3}. In the residual geoid map (contour, interval ~ 0.25m), different tectonic features could be identified e.g. the eastern continental margin of India, the Bengal Fan, the Ninetyeast and 85°E Ridges, the Andaman Trench⁴.

The age data has been considered from the published isochron data (Müller *et al.*¹²). An age comparison of the Arabian Basin with BOB shows that the Arabian basin is the youngest with minimum age nearing zero Myr as seen over the spreading Carlsberg Ridge and a maximum age of 81 Ma at the southernmost portion in off-continental shelf of Pakistan.

Age of the Northern Indian Ocean lithosphere: The age contours over the Bay of Bengal are showing two major steps like shift over both the Ninetyeast and 85°E Ridges. The age value increases as one move from Sumatran trench region to the north-west of the Bay of Bengal near eastern coast of India (Fig. 2).

From the whole set of altimeter profiles we have taken only two ridge zones (85°E Ridge and Ninetyeast Ridge) over the Bay of Bengal. The residual geoid anomalies were plotted over these two regions and measured on a certain profile along a particular latitude (Fig. 3). The age offset were estimated in addition to the residual geoid offset. All these profiles are shown in Figs 4a and b. The residual geoid offsets over 85°E Ridge have been measured



RESIDUAL GEOID OVER INDIAN OFFSHORE USING HIGH RESOLUTION ALTIMETER DATA BASE

REFER THIS MAP AS:

PROJECTION : MERCATOR

SPHEROID: WGS 84

CENTRAL MERIDIAN: 80 E

SCALE 1: 15,000,000

CONTOUR INTERVAL : 0.25 m.

0 250 500 1,000 Kilometers

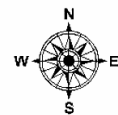


Fig. 1—Residual Geoid over Indian offshore using high resolution satellite altimeter data.

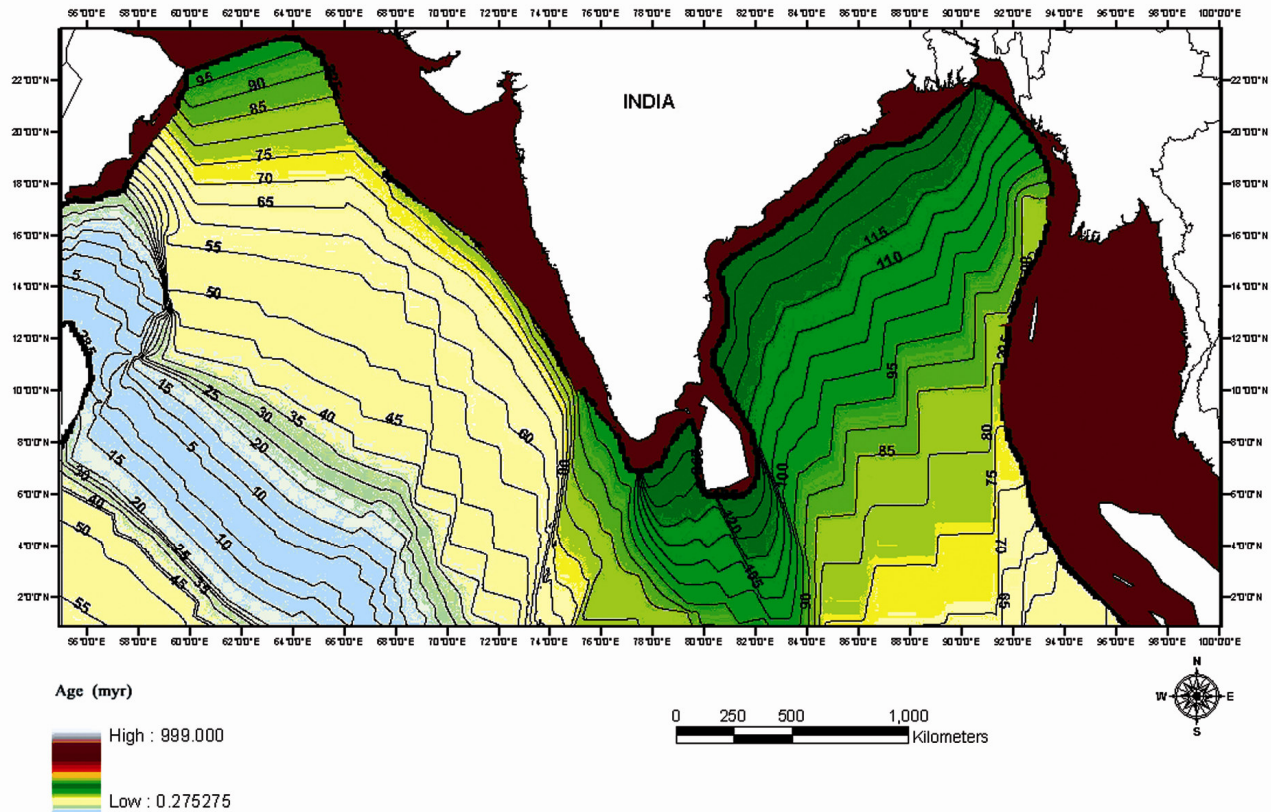


Fig. 2—Age contour map over the Indian Ocean (after Müller *et al.*¹²)

between longitudes 83°E to 88°E and latitudes 5°N to 18°N whereas the residual geoid offsets over the Ninetyeast Ridge have been measured between longitudes 89°E to 91°E and latitudes 5°N to 17°N. The age offset also has been measured between the same latitude and longitude.

The present study consists of a part of the 85°E Ridge between longitudes 83°E to 88°E. The length of the data segments had been limited to the part which crosses the 85°E ridge. Simultaneously, residual geoid data have been considered for each profile, after removal of wavelengths due to deeper earth effects. The effects on the lithospheric flexure at fracture zones, ridge areas have not yet been investigated properly over the Bay of Bengal. It is quite plausible that the observed shape of the residual geoid anomaly results from this phenomena. In the absence of a quantitative study, it has been considered simultaneously two measures (Figs. 4a and b): (1) offset of the regional trend and (2) local step from the lowest low to highest high⁷. This geoid offset had been estimated using residual geoid data. In a similar fashion, the age offset from the age contours have been observed. (Figs. 5 a and b).

Geoid models for ocean ridges and fracture zones

If $h(t)$ is the slope is the geoid as a function of seafloor age, resulting from changes in seafloor depth and plate thickness due to cooling, then the quantity ($\Delta h/\text{age}$ offset) estimated above is simply the derivative of $h(t)$ with respect to age, where t is the mean age between two sides of a fracture⁸. From the geoid data, it is possible to estimate $h(t)$ and its derivative using the residual geoid anomalies. Haxby and Turcotte⁹ have derived a theoretical expression for the geoid anomaly caused by lithospheric cooling, assuming that the isostatic equilibrium prevails at the base. If the ridge crest is taken as reference, then the 'isostatic' geoid anomaly as a function of age t is^{7,8}.

$$h(t) = -2\pi G/g \left\{ (\rho_m - \rho_w)/2 w(t)^2 - \alpha \rho_m \int (w(t) + z) [T_m - T(z, t)] dz \right\} \dots (1)$$

where, G = gravitational constant; g = mean surface gravity; α = volume coefficient of thermal expansion; ρ_m = density of mantle rock at temperature T_m ; ρ_w = density of sea water; $w(t)$ = subsidence of plate referred to the ridge crest and scaled to the plate thickness H ; T_m = bottom boundary temperature; $T(z, t)$ = temperature inside the slab at depth z (positive downward) and age t .

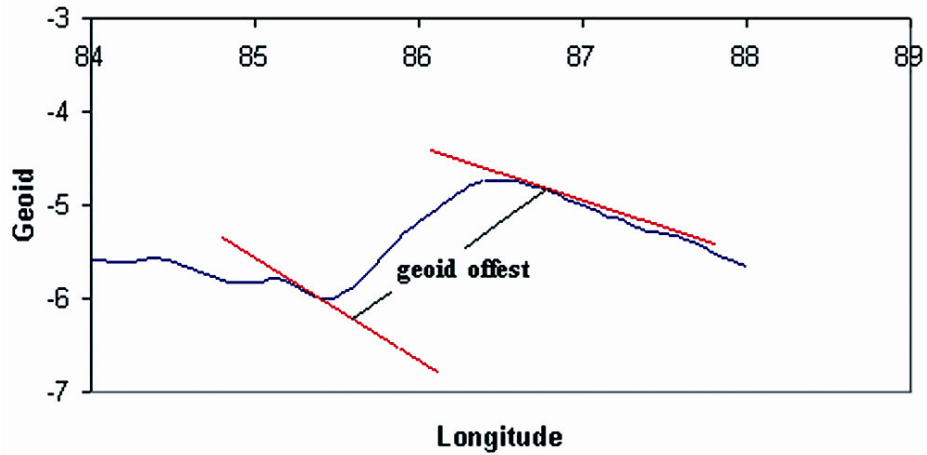


Fig. 3—Estimation of geoid offset along a geoid profile.

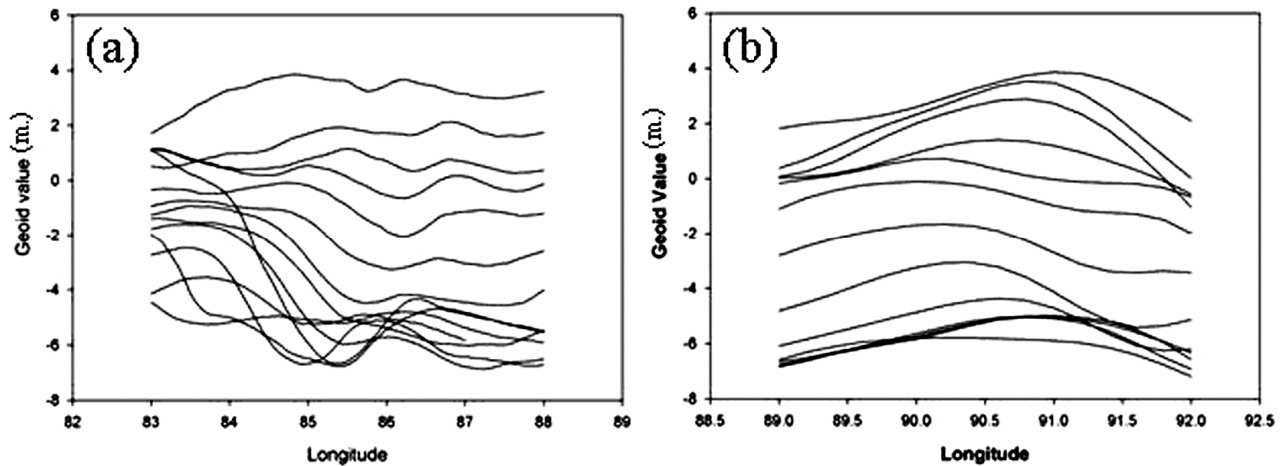


Fig. 4—Geoid offsets over (a) 85°E Ridge, (b) Ninetyeast Ridge.

For the ‘plate’ cooling model, expressions for $T(z, t)$ and $w(t)$ are⁶:-

$$T(z, t) = T_m \left\{ \frac{z}{H} + \frac{2}{\pi} \sum_{n=1}^{\infty} \frac{1}{n} [\sin(n \pi z/H) \exp(-\beta_n ut/H)] \right\} \dots (2)$$

with $\beta_n = \{(R^2 + n^2 \pi^2)^{1/2} - R\}$, $R = u H / (2 \kappa)$, and

$$w(t) = \alpha \rho_m T_m / 2 (\rho_m - \rho_w)^{-1} \left[1 - \frac{8}{\pi^2} \sum_{n=1}^{\infty} \exp(-\beta_{2n-1} ut/H) (2n - 1)^{-2} \right] \dots (3)$$

where, u = spreading velocity, and κ = thermal diffusivity.

For the plate model, solution (3) is similar at all smaller ages. They give a very good agreement with the observed trend in seafloor depth ages less than 60-80 Ma. For larger ages, the seafloor topography follows rather the behavior predicted by the plate model in approaching towards a constant depth^{6,13}.

Physically, this indicates that an additional source of heat is introduced at the base of the lithosphere. Substituting expressions for ocean depth and temperature distribution given above for the plate models, $h(t)$ can be expressed as⁸.

$$h(t) = -2\pi G H^2 / g \left\{ (\rho_m - \rho_w) w(t)^2 / 2 + \alpha \rho_m T_m [1/6 + 2/\pi^2 \sum Q_n] \right\} \dots (4)$$

where $Q_n = (-1)^n / n^2 \exp(-\beta_n ut/H)$ and $w(t)$ given in equation (3).

Thus the plate model predicts that the geoid height decreases much more slowly and approaches asymptotically a constant value at large ages (like seafloor depth).

The theoretical changes in geoid height with age associated with the plate models were computed, for different values of these parameters α , κ , T_m , and H . We have also computed the derivative of $h(t)$ with

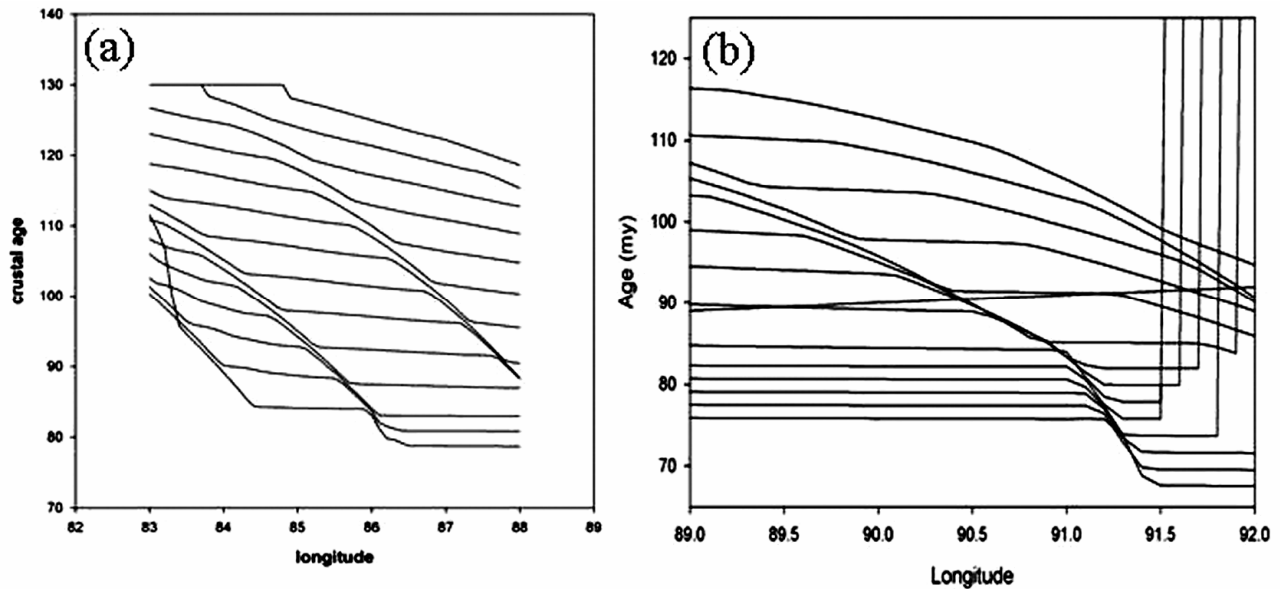


Fig. 5—Age offsets over (a) 85°E Ridge, (b) Ninetyeast Ridge.

respect to t , since as discussed above; geoid anomalies of fracture zones give this function directly. In the case of the plate model, on the contrary the derivative $\Delta h/\Delta t$ is a function of age¹⁴.

Theoretical curves for $h(t)$ and $\Delta h/\Delta t$ have been calculated for different sets of parameters (α , κ , T_m and H). The numerical values used are:

$\kappa = 0.8, 1.0, 1.2, 1.5$ ($10 \text{ cm}^2 \text{ s}^{-1}$); $\alpha = 3.0, 3.2, 3.4, 3.6$ ($10^{-5} \text{ }^\circ\text{C}^{-1}$); $T_m = 1200, 1350, 1500, 1700$ ($^\circ\text{C}$); $H = 50, 75, 100, 125$ (km)

For other parameters, we have used $\rho_m = 3.33 \text{ g cm}^{-3}$, $\rho_w = 1.03 \text{ g cm}^{-3}$, and $g = 980 \text{ cm s}^{-2}$ with spreading velocity u : 1 and 8 cm yr^{-1} . However, $h(t)$ and $\Delta h/\Delta t$ appear insensitive to u which can be demonstrated easily from the theoretical expressions of h/t and $\Delta h/\Delta t$ curves for the plate model. A number of features appear from the curves as shown in Fig. 6: (a) $\Delta h/\Delta t$ decreases rapidly with age at small values of the lithospheric thickness; (b) At small ages, $\Delta h/\Delta t$ is independent of H ; (c) At small ages, the effects of changes of the parameters κ , α , T_m and are equivalent^{7,8}.

To summarize, the value of $\Delta h/\Delta t$ near the origin is related to the combined values of κ , α , and T_m , while its overall trend is mainly related to the thickness H with the increase in age. Points (a) and (b) can be seen easily from the derivative of relation (4): for $t = 0$,

$$\Delta h/\Delta t \approx -2 \pi G/g \alpha \rho_m T_m \kappa \dots (5)$$

For larger t ,

$$\Delta h/\Delta t \approx -4 \pi G/g \alpha \rho_m T_m \kappa \exp(-\pi^2 \kappa t/H^2) \dots (6)$$

Hence κ , α , and T_m play the same role near the origin.

Estimation of lithospheric thicknesses

The modeled curves computed with $\omega (= \alpha \kappa T_m)$ $0.52 \times 10^{-3} \text{ cm}^{-2} \text{ s}^{-1}$ (Fig. 6) and different H values indicates that a single model curve can hardly explain all observed $\Delta h/\Delta t$. The geoid offset/age ratio have been plotted for two different regions of the Bay of Bengal (85°E Ridge and Ninetyeast Ridge). Observed values of these two graphs fit with the theoretically derived geoid offset/age value for two different H values (plate thicknesses). Observed values of ($\Delta h/\Delta t$ offset) are shown in Figs 7 and 8 as function of age. Table 1 shows the observed geoid offset and age offset values over the two fracture zones and also the geoid offset/age offset ratios. Figures 6 and 7 indicate that the observed geoid offset/age value resembles with the computed $\Delta h/\Delta t$ versus age curve, when the lithospheric thickness (H) is 100 km; whereas for Fig. 8, it matches with the lithospheric thickness of 125 km. Figures 7 and 8 elucidate that the lithospheric thicknesses below the 85°E Ridge and the Ninetyeast Ridge are around 100 km and 125 km respectively.

Results and Discussion

The oceanic crust in the Bay of Bengal was formed during the early Cretaceous and traversed by two

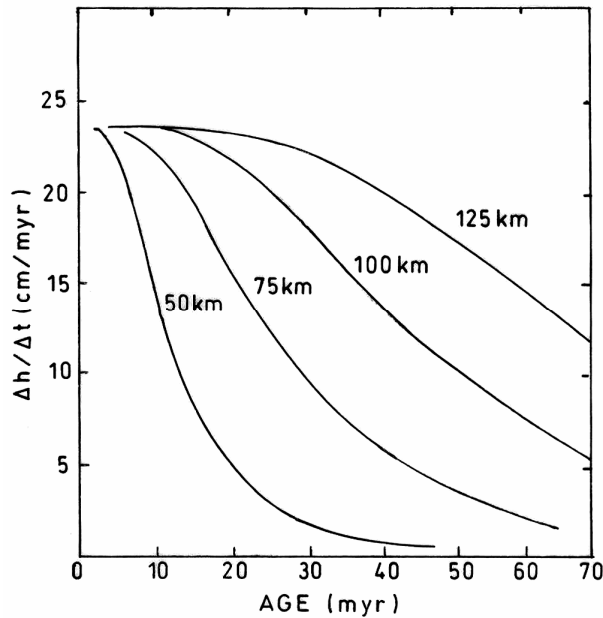


Fig. 6—Computed $\Delta h/\Delta t$ versus age for $H = 50, 75, 100, 125$ km.

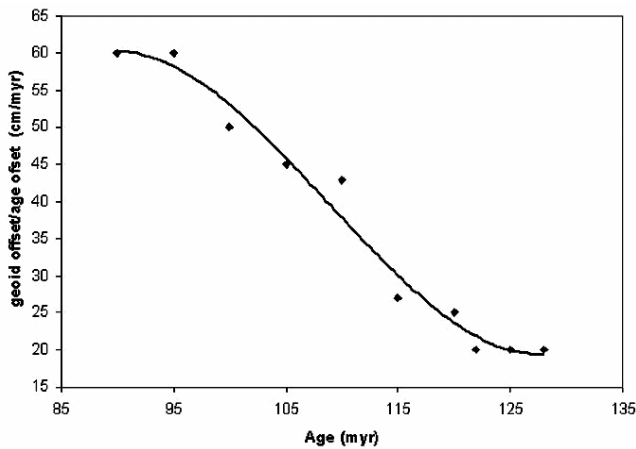


Fig. 7—Observed $\Delta h/\Delta t$ versus age over the 85°E Ridge.

major volcanic features as the Ninetyeast and the 85°E Ridges. The Bengal Fan is thus divided into two basins, Western Basin (between the eastern margin of India and the 85°E Ridge), and the Central Basin (between the 85°E and the Ninetyeast Ridges).

The 85°E Ridge — Afanasy Nikitin Seamount (ANS) system is an aseismic ridge system which extends for about 2600 km in the N-S direction between 19°N and 5°S. The 85°E Ridge is a typical enigmatic feature and its morphology varies all along the ridge. Most of the 85°E Ridge was formed during the mid cretaceous Ma. It is clear from its trends of volcanic traces and fracture zones of the north Indian Ocean that during the mid-Cretaceous – early Tertiary

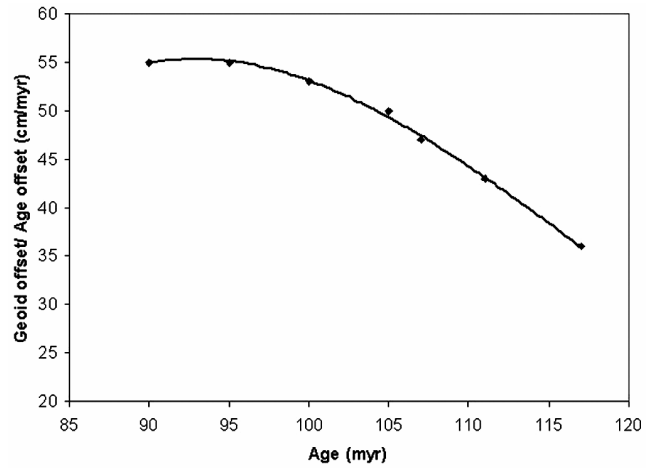


Fig. 8—Observed $\Delta h/\Delta t$ versus age over the Ninetyeast Ridge.

period, the Indian plate was in N-S directional motion¹⁵⁻¹⁷. The oceanic crust formed in the Bay of Bengal in two different phases (NW-SE and N-S) during mid-Cretaceous¹⁸. The N-S trend of the 85°E Ridge and cessation of volcanism in the vicinity of the Afanasy Nikitin Seamount (southern portion of the 85°E Ridge) suggest that the hotspot had formed the entire ridge system (85°E Ridge, buried hills and Afanasy Nikitin Seamount (ANS)) some time in the middle Cretaceous to Paleocene age. In other words, the hotspot initiated volcanism ~ 85 Ma in the northern Bay of Bengal and ended in the vicinity of the ANS ~ 55 Ma. The emplacement of the ANS near a ridge crest and initial volcanism of the 85°E Ridge appear to be contemporary event of ~ 85Ma. Low-density material is associated with the 85°E Ridge. The free-air gravity anomaly pattern also changes from low to high gravity while moving from the north to the south of this ridge¹⁹.

Several studies have been carried out to find the lithospheric structure of the Bay of Bengal and central Indian Ocean through satellite-derived geoid and gravity²⁰⁻²¹ as well as surface wave analyses of regional and teleseismic waveforms recorded over some broad band seismic network in southern India and also permanent stations on the Indian Ocean islands²²⁻²³. Most of the surface wave paths represent pure ocean character. The study shows that the thickness of lithosphere of the southern part of the Bay of Bengal is greater than 70 km²². The Qbeta-1 models show a lithosphere thickness of 120 km is estimated beneath the Bay of Bengal Fan, and lithosphere thicknesses between 100 and 80 km beneath the Indian Ocean off- and across Ninetyeast

Table 1—Observed geoid and age offset values over the 85°E and the Ninetyeast ridges

Ridge Zone	Latitude (°N)	Geoid Offset (m)	Age Offset (Myr)	(Geoid Offset/ Age Offset)*
85°E ridge	08.00	4.8	8	60
85°E ridge	09.00	4.8	8	60
85°E ridge	10.00	4.5	9	50
85°E ridge	11.00	4.5	10	45
85°E ridge	12.00	3.5	8	43
85°E ridge	13.00	2.0	7	27
85°E ridge	14.00	2.0	7	25
85°E ridge	15.00	1.0	5	20
85°E ridge	16.00	1.0	5	20
85°E ridge	17.00	1.0	5	20
90°E ridge	12.00	2.7	5	55
90°E ridge	13.00	2.7	5	55
90°E ridge	14.00	2.6	5	53
90°E ridge	15.00	2.5	5	50
90°E ridge	16.00	2.8	6	47
90°E ridge	17.00	3.0	7	43
90°E ridge	18.00	2.5	7	36

Ridge respectively²³. Geoid vs. age offset curves below the 85°E and the Ninetyeast Ridges show lithospheric thicknesses of around 100 km and 125 km respectively which tally the observations of Qbeta-1 models²³.

Conclusions

The results of the present study (similarity of lithospheric thickness derived from the calculated and observed geoid vs. age offset ratio) show the effectiveness of using the plate model over the Bay of Bengal for estimation of the lithospheric thickness. The high-resolution geoid database (off-track resolution: 3.33 km) have increased the accuracy of the observed geoid offset value. Other studies like surface wave analysis²¹ and inversion of Love and Raleigh wave attenuation data²³ have estimated the similar lithospheric thicknesses in this region. It may be concluded that the plate thicknesses derived for these two regions reflects local thermal anomalies and are not at all representatives of the average thickness of the total Bay of Bengal oceanic lithosphere. Further analyses, like the one given here, should be extended to other oceanic regions of the Bay of Bengal and also to the Arabian Sea. These will possibly reveal the changes in lithospheric thickness and the identification of lithospheric undulation from this high resolution satellite geoid database. Due to the prevailing security restrictions, lat./lon. markings have been omitted in Fig. 1.

Acknowledgements

The authors are very much thankful to Prof. C. Hwang, National Chiao Tung University, Taiwan for providing high-resolution geoid/gravity data and the related software. They are also thankful to Dr. R. R. Navalgund, Director, SAC, Dr. S. R. Shetye, Director, NIO, Dr. J. S. Parihar, DD, RESA, and Dr. Ajai, GD, MESG for their keen interest in this study.

References

- 1 Biswas S K, Rift basins in western margin of India and their hydrocarbon prospects with special reference to Kutch Basin, *Amer Assoc Petr Geol Bull (AAPG)*, 66 (1982) 1497-1513.
- 2 Majumdar T J, Mohanty K K & Srivastava A K, On the utilization of ERS-1 altimeter data for offshore oil exploration, *Int J Remote Sens*, 9 (1998) 1953-1968.
- 3 Hwang C, Hsu H Y & Jang R J, Global mean surface and marine gravity anomaly from multi-satellite altimetry: application of deflection-geoid and inverse Vening Meinesz formulae, *J Geodesy*, 76 (2002) 407- 418.
- 4 Majumdar T J & Bhattacharyya R, *An Atlas of very high resolution satellite geoid/gravity over the Indian offshore*, SAC Tech. Note No. SAC/RESIPA/MWRG/ESHD/TR-21/2004 (Space Applications Centre, Ahmedabad, India) 2004.
- 5 Lundgren B & Nordin P, Satellite altimetry - a new prospecting tool, *Proc. 6th Thematic Conference*, Colorado, Environmental Research Institute of Michigan (USA), Ann Arbor, Michigan (1988), pp 565-575.
- 6 Parsons B & Sclater J G, An analysis of the variation of ocean floor bathymetry and heat flow with age, *J Geophys Res*, 82 (1977) 803-827.
- 7 Cazenave A, Lago B, Dominh K & Lambeck K, On the response of the ocean lithosphere to seamount loads from GEOS 3 satellite radar altimeter observations, *Geophys J R Astron Soc*, 63 (1980) 233-252.
- 8 Cazenave A, Lago B & Dominh K, Thermal parameters at the oceanic lithosphere estimated from geoid height data, *J Geophys Res*, 88 (1983) 1105-1118.
- 9 Haxby W F & Turcotte D L, On isostatic geoid anomalies, *J Geophys Res*, 83 (1978) 5473-5478.
- 10 Parsons B & Richter F M, A relation between the driving force and geoid anomaly associated with mid-ocean ridges, *Earth & Planet Sci Lett*, 51 (1980) 445-450.
- 11 Sandwell D & Schubert G, Geoid height versus age for symmetric spreading ridges, *J Geophys Res*, 85 (1980) 7235-7241.
- 12 Müller R D, Roest W R, Royer J Y, Gahagan L M & Sclater J G, Digital isochrons of the world's ocean floor, *J Geophys Res*, 102 (1997) 3211-3214.
- 13 Sclater J G, Jaupart C & Galson D, The heat flow through oceanic and continental crust and the heat loss of the earth, *Rev Geophys Phys*, 18 (1980) 269-311.
- 14 Crough S T, Geoid anomalies across fractures zones and the thickness of the lithosphere, *Earth & Planet Sci Lett*, 44 (1979) 224-230.

- 15 Ramana M V, Subrahmanyam V, Chaubey A K, Ramprasad T, Sarma K V L N S, Krishna KS, Desa M & Murty GPS, Structure and origin of the 85° E ridge, *J Geophys Res*, 102 (1997) 17995-18012.
- 16 Liu C S, Sandwell D T & Curray J R, 1982, The negative gravity anomaly over 85° E ridge, *J Geophys Res*, 87 (1982) 7673-7686.
- 17 Subrahmanyam V, Krishna K S, Radhakrishna Murthy I V, Sarma K V L N S, Desa M, Ramana MV & Kamesh Raju KA, Gravity anomalies and crustal structure of the Bay of Bengal, *Earth & Planet Sci Lett*, 192 (2001) 447-456.
- 18 Krishna K S, Laju M, Bhattacharyya R & Majumdar T J, Geoid and gravity anomaly data of conjugate regions of Bay of Bengal and Enderby Basin : new constraints on breakup and spreading history between India and Antarctica, *J Geophys Res*, 114 (2009) B03102, doi:10.1029/2008JB005808, 21 p.
- 19 Krishna K S, Structure and evolution of the Afanasy Nikitin seamount, buried hills and 85°E Ridge in the northeastern Indian Ocean, *Earth & Planet Sci Lett*, 209 (2003) 379-394.
- 20 Majumdar T J, Krishna K S, Chatterjee S, Bhattacharyya R & Michael L, Study of high-resolution satellite geoid and gravity anomaly data over the Bay of Bengal, *Curr Sci*, 90 (2006) 211-219.
- 21 Rajesh S & Majumdar T J, Geoid generation and subsurface structure delineation under the Bay of Bengal, India using satellite altimeter data, *Curr Sci*, 84 (2003) 1428-1436.
- 22 Chandra S, Wu F T & Rai S S, Seismic surface wave imaging of the Indian Ocean. <http://www.nio.org/jsp/tsunami.jsp> (last accessed 23.8.07).
- 23 Singh D D, Q-structure beneath the north and central Indian Ocean from the inversion of observed Love and Raleigh wave attenuation data, *Phys Earth and Planet Int*, 59 (1990) 243-258.